Analyzing power of $^{206}Pb(\vec{p},p_0)$ and $^{207}Pb(\vec{p},p_0)$ near the $3p_{1/2}$ isobaric analog resonance

N. L. Back, M. P. Baker,* J. G. Cramer, and T. A. Trainor
University of Washington, Seattle, Washington 98195
(Received 26 September 1977)

The $3p_{1/2}$ isobaric analog resonances in the compound nuclei ^{207}Bi and ^{208}Bi have been studied by measuring the cross sections and analyzing powers of the reactions $^{206}Pb(\vec{p},p_0)$ and $^{207}Pb(\vec{p},p_0)$. The data were fitted with an optical-model background and Breit-Wigner resonance terms. The resonance energies, elastic partial widths, and elastic mixing phases were extracted. The elastic partial widths are significantly different from those previously determined from differential cross-section measurements. The previously measured inelastic partial widths were adjusted to account for this difference. In the case of the isobaric analog state in ^{208}Bi, the results are inconsistent with a recent theoretical treatment of the isobaric analog state as a single broad pole in the energy-averaged S matrix.

[NUCLEAR REACTIONS $^{206,207}Pb(\vec{p},p)$, $E=10$–13.6 MeV; measured $\sigma(E;\theta)$, $A(E;\theta)$; deduced optical-model parameters. ^{207,208}Bi IAS, deduced energy, partial width, mixing phase.]

I. INTRODUCTION

Since the discovery of isobaric analog resonances (IAR) in heavy nuclei, much attention has been focused on these resonances in the "double magic" lead region because of the success of the nuclear shell model in describing nuclear structure there. Most of the attention, however, has centered on the positive parity states above the ^{208}Pb shell closure. Previous studies of the p-wave IAR in the reactions $^{206}Pb+p$ and $^{207}Pb+p$ have measured only differential cross sections.[1-3] Since the p-wave resonances are excited at energies well below the Coulomb barrier the dominant contribution to elastic scattering is from Rutherford scattering and the resonance amplitude appears only as a small perturbation on the dominant Rutherford amplitude.

On the other hand, one can obtain additional independent information on the resonance by measuring the analyzing power of the reaction as well as the cross section. This is most easily accomplished with a polarized proton beam. Because the analyzing power is linear in the resonance amplitude and because it is possible to find scattering angles at which the analyzing power due to potential scattering is essentially zero, it is possible to obtain high quality information on the parameters of the IAR.

The analyzing power of the reactions $^{206}Pb(\vec{p},p_0)$ and $^{207}Pb(\vec{p},p_0)$ has been measured in the vicinity of the isobaric analogs of the ground states of ^{207}Pb and ^{208}Pb, respectively. The resonance energies, elastic partial widths, and elastic mixing phases were determined by fitting the data with optical model background and Breit-Wigner resonance amplitudes. The resulting partial widths were found to be different from those previously determined from cross section measurements. In addition, the mixing phases were found to be small, in agreement with similar studies in medium-weight nuclei.[4]

II. EXPERIMENTAL PROCEDURE

The polarized proton beam was produced by the University of Washington Lamb-shift polarized ion source and accelerated by the laboratory's FN tandem Van de Graaff accelerator. The beam was analyzed and directed to a 152.4 cm diameter scattering chamber. For the $^{206}Pb(\vec{p},p_0)$ runs, the target was isotopically enriched (>97%) self-supporting ^{206}Pb with a thickness of approximately 400 $\mu g/cm^2$. The scattered protons were detected by three pairs of symmetrically placed Si(Li) detectors, and by a monitor detector at a lab angle of 30°. In addition, the beam polarization was continuously monitored by a ^{4}He polarimeter: protons elastically scattered by ^{4}He in a gas target were detected by a pair of Si(Li) detectors at a lab angle of 112°. For the $^{207}Pb(\vec{p},p_0)$ runs, the setup was essentially the same, except that (a) there was no monitor, and (b) the target was 520 $\mu g/cm^2$ of isotopically enriched (>92%) ^{207}Pb on a 20 $\mu g/cm^2$ carbon backing. The angular acceptance of the detectors was about ±2° for the ^{206}Pb runs, and about ±1° for the ^{207}Pb runs. The uncertainty in the beam energy is estimated to be about 1 keV (based on the uncertainty in the calibration of the analyzing magnet).

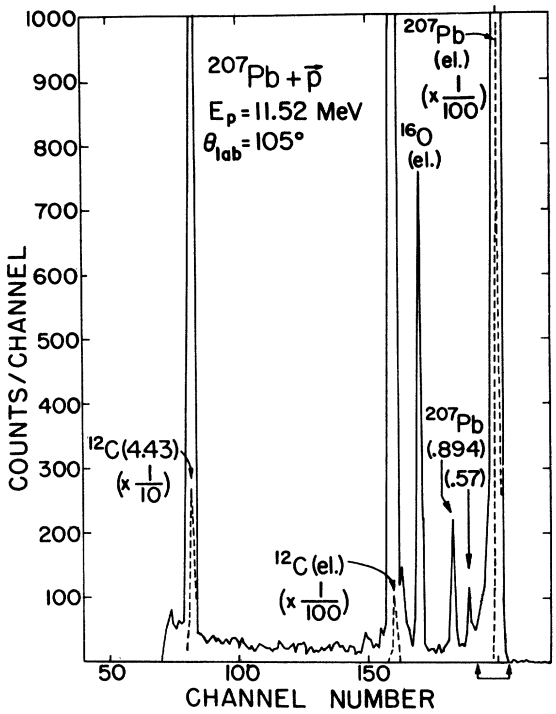

FIG. 1. Typical on-resonance spectrum for ^{207}Pb+$\vec{p}$. The bracket indicates the channels used for integration of the elastic peak.

A typical on-resonance spectrum for ^{207}Pb is shown in Fig. 1. In addition to the elastic peak, two inelastic peaks, corresponding to the $\frac{5}{2}^-$ (0.570 MeV) and $\frac{3}{2}^-$ (0.894 MeV) states in ^{207}Pb, are clearly visible. Away from the resonance, these two peaks cannot be distinguished from the background. Similar spectra are seen for ^{206}Pb, except that the lowest excited state is the 2^+ (0.803 MeV) state. Due to improvements in the polarized ion source between the ^{206}Pb and ^{207}Pb runs, the beam intensity and hence the number of counts was greater for the latter; the statistical uncertainties in the elastic peak sums are about 1% and 0.5%, respectively.

The polarization and analyzing power were found by taking two consecutive runs, one with spin up and the other with spin down. Thus, at each angle there were four peak sums, which we call $L\uparrow$, $L\downarrow$, $R\uparrow$, and $R\downarrow$. We use the formula

$$pA(\theta)=\frac{1-r}{1+r}\,, \quad \text{where } r=\left(\frac{L\uparrow R\downarrow}{L\downarrow R\uparrow}\right)^{1/2}. \tag{1}$$

In this way, false asymmetries due to geometrical factors and beam integration uncertainty are eliminated.

For ^{206}Pb($\vec{p},p_0$), the analyzing power excitation function was measured from 11.00 to 13.60 MeV in 100 keV steps, except that measurements were

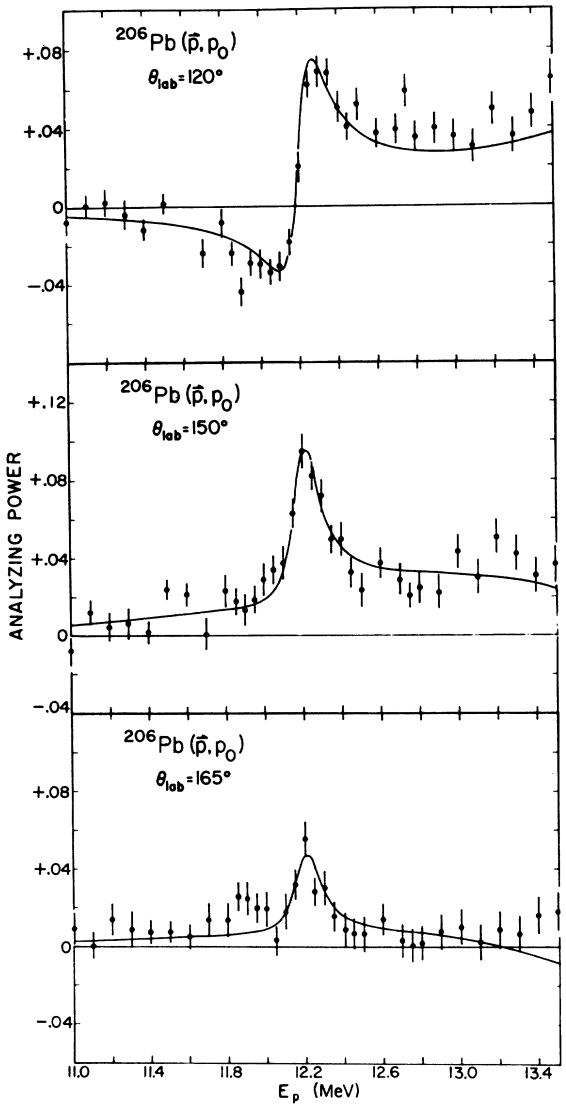

FIG. 2. Analyzing-power excitation functions for ^{206}Pb($\vec{p},p_0$) at θ_{lab}=120°, 150°, and 165°. The curves are generated from the optical-model and resonance parameters given in Tables I and II.

made in 50 keV steps near the resonance. The angles used were 120°, 150°, and 165°. The resonant structure is visible at all three angles, as can be seen in Fig. 2. In addition, angular distributions for both the analyzing power and the differential cross section were measured at 11.50 and 12.75 MeV. These are shown in Fig. 3.

For ^{207}Pb($\vec{p},p_0$), the analyzing power excitation function was measured from 11.00 to 12.10 MeV in 50 keV steps, except near the resonance, where smaller steps were used. The angles used were 105°, 120°, and 135°. The data (shown in Fig. 4) are actually a combination of two runs taken a

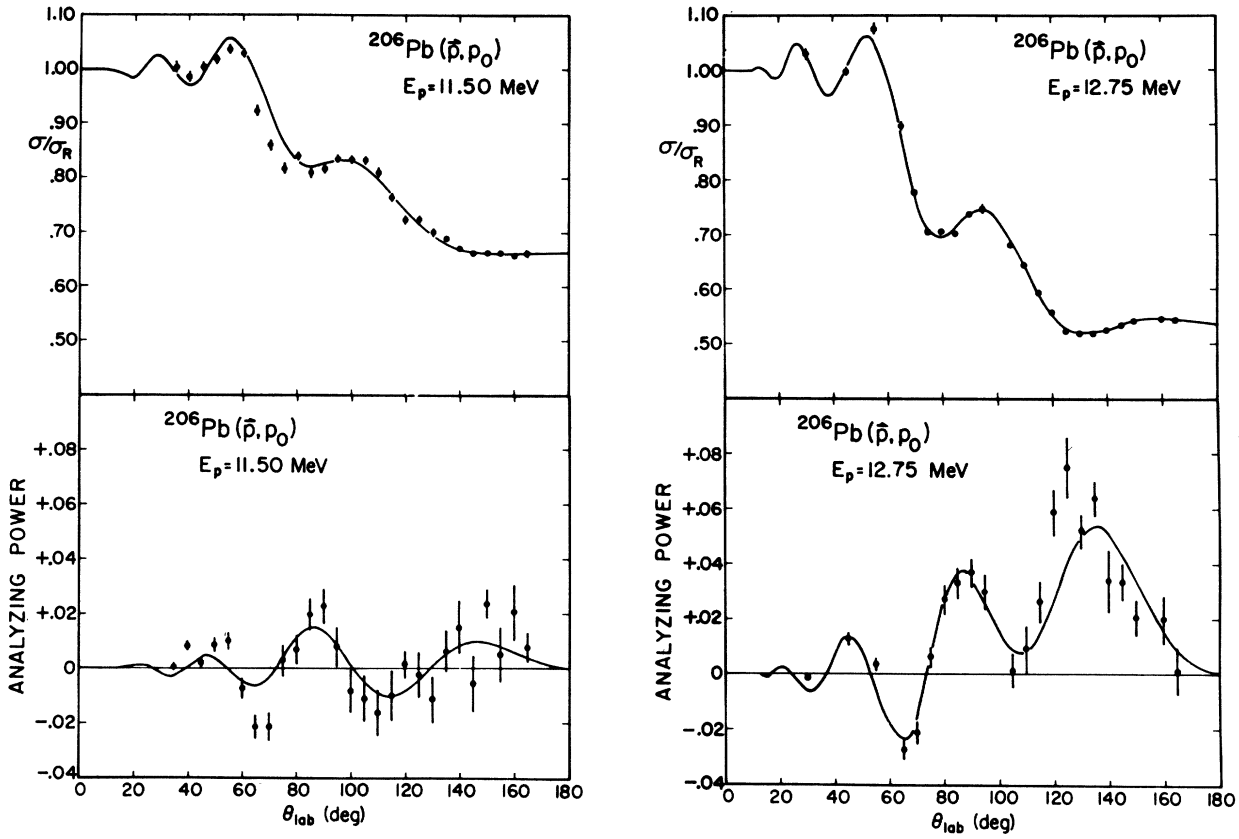

FIG. 3. Differential cross-section and analyzing-power angular distributions for $^{206}Pb(\vec{p},p_0)$ at two off-resonance energies, $E_p = 11.50$ and 12.75 MeV. The curves are generated with the optical-model parameters in Table I.

month apart as a consistency check. Figure 5 shows the angular distributions, measured in this case at 10.00 and 13.00 MeV. A tabulation of the data has been deposited in the Physics Auxiliary Publications Service.[5]

III. ANALYSIS

The elastic scattering of a proton in the vicinity of an isolated IAR can be described in terms of an average S matrix[6]:

$$\langle S_{cc}\rangle = \langle S_{cc}\rangle_{BG} + \langle S_{cc}\rangle_{RES} , \tag{2}$$

where

$$\langle S_{cc}\rangle_{RES} = -ie^{2i\delta_c} \frac{\Gamma_{0c} e^{2i\phi_c}}{E - \epsilon_0 + \frac{1}{2} i\Gamma_0} \tag{3}$$

and

$$\langle S_{cc}\rangle_{BG} = e^{2i\delta_c} e^{-2\eta_c} . \tag{4}$$

Here, ϵ_0 and Γ_0 are the energy and width of the IAR, Γ_{0c} and $2\phi_c$ are the magnitude and phase of the complex partial width $\tilde{\Gamma}_{0c}$, and $\delta_c + i\eta_c$ is the complex phase shift for the background scattering. While many channels can contribute to the background, the IAR can occur only in the channel $c = \{L,J,I\}$ (where L,J refer to the incoming partial wave and I to the total angular momentum). More generally, one might consider the effect of other resonances which, though outside the energy region of interest, have a large enough width that they cannot be ignored. As long as no two IAR have the same spin and parity, there will be no mixing between them, and each one can be considered separately. Thus there may be several channels which have $\langle S_{cc}\rangle_{RES} \neq 0$. The background phase shifts can be calculated using the optical model. They consist of the Coulomb phase shifts σ_l and the nuclear phase shifts $\Delta_c = \lambda_{lj} + i\eta_{lj}$, so that

$$\langle S_{cc}\rangle_{BG} = e^{2i\sigma_l} e^{2i\Delta_c} = e^{2i(\sigma_l + \lambda_{lj})} e^{-2\eta_{lj}} . \tag{5}$$

If the fluctuating part of the average cross section is negligible, then the average differential cross section and analyzing power are given by[7]:

$$\frac{d\sigma}{d\Omega}(E,\theta) \approx |\alpha(E,\theta)|^2 + |\beta(E,\theta)|^2 , \tag{6}$$

$$A(E,\theta)\frac{d\sigma}{d\Omega}(E,\theta) \approx -2\,\mathrm{Im}[\alpha(E,\theta)\beta^*(E,\theta)] , \tag{7}$$

where

$$\alpha(E,\theta)=f_c(E,\theta)+\frac{1}{2ik}\sum_{l=0}^{\infty}\sum_{j=l-\frac{1}{2}}^{l+\frac{1}{2}}(j+\tfrac{1}{2})(\langle S_{cc}\rangle_{BG}-e^{2i\sigma_l})P_l(\cos\theta)+\frac{1}{2ik}\sum_{RES}\frac{(2l+1)}{(2I_0+1)(2J+1)}(J+\tfrac{1}{2})\langle S_{cc}\rangle_{RES}P_L(\cos\theta)\,, \tag{8}$$

and

$$\beta(E,\theta)=\frac{1}{2ik}\sum_{l=1}^{\infty}\sum_{j=l-\frac{1}{2}}^{l+\frac{1}{2}}(-1)^{l-j+\frac{1}{2}}\langle S_{cc}\rangle_{BG}P_l^1(\cos\theta)+\frac{1}{2ik}\sum_{RES}\frac{(2l+1)}{(2I_0+1)(2J+1)}(-1)^{L-J+\frac{1}{2}}\langle S_{cc}\rangle_{RES}P_L^1(\cos\theta)\,. \tag{9}$$

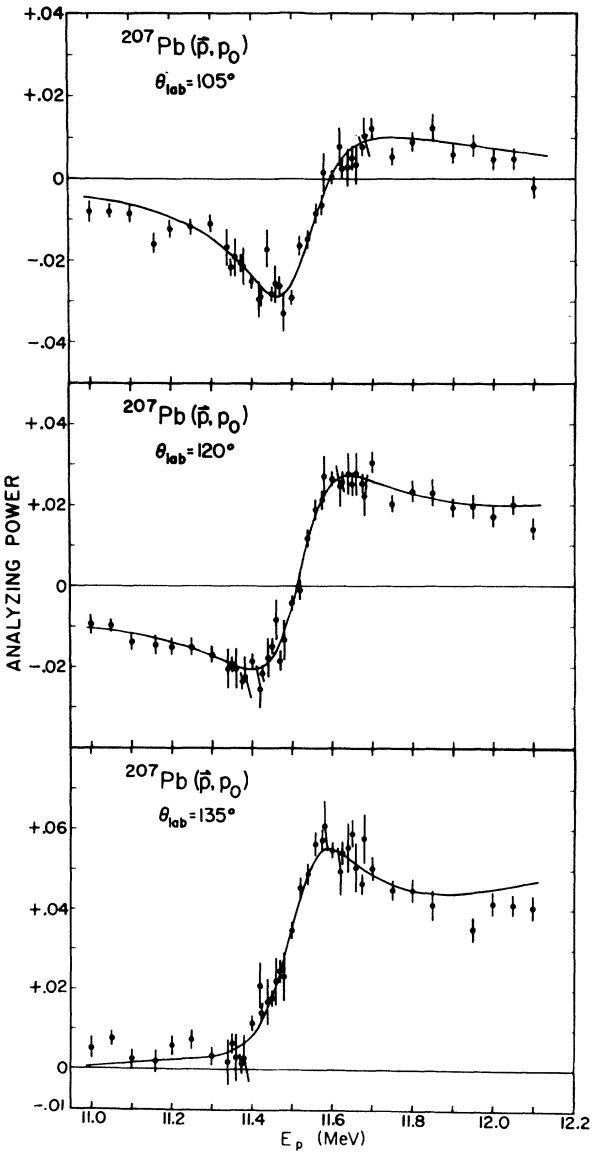

FIG. 4. Analyzing-power excitation functions for ^{207}Pb($\vec{p}$,p_0) at θ_{lab}=105°, 120°, and 135°. The curves are generated from the optical-model and resonance parameters given in Tables I and II.

These formulas are exact if the target spin I_0 is zero (which is the case for ^{206}Pb), and are approximately true for $I_0=\frac{1}{2}$ (e.g., ^{207}Pb) with small corrections needed near the resonance energies.

The optical potential used was of the standard form,[8] with linear energy dependences for the real and imaginary potentials, a spin-orbit term of the Thomas form, and a surface-peaked imaginary potential. Initially, a set of optical model parameters determined by Rathmell and Haeberli[9] for polarized proton scattering from ^{207}Pb and ^{208}Pb at 13 MeV were used (the ^{208}Pb parameters were used for ^{206}Pb). However, these parameter sets did not give a very good fit either to the angular distributions or to the off-resonance parts of the excitation functions. Therefore, it was necessary to search for the sets of parameters that would give the best fits to the measured angular distributions. For the search, the optical model code GENOA was used,[10] with appropriate modifications to take the resonances into account. The best estimates of the $p_{1/2}$ resonance parameters (based on preliminary analyses of the excitation-function data) were used. Also included were the following: (a) for ^{206}Pb, the higher-lying $g_{9/2}$, $i_{11/2}$, $d_{5/2}$, $s_{1/2}$, $g_{7/2}$, and $d_{3/2}$ IAR, using the resonance parameters for the corresponding IAR in ^{208}Pb (Ref. 11); (b) for ^{207}Pb, the 5^- IAR, with the parameters found by Ramavataram *et al.*[12] (except that ϕ_c was set equal to zero). Since the resonance parameters were not changed by the optical model program, an iterative technique was required. That is, the best fit to the angular distributions was determined with the initial set of resonance parameters, then the new optical model set was used to obtain a better estimate of the $p_{1/2}$ resonance parameters, and so on until a set of optical-model and resonance parameters was found that would give a reasonably good fit to all the data.

The ^{206}Pb and ^{207}Pb angular distributions were analyzed separately. In each case, the program was allowed to vary all parameters except the Coulomb radius r_C and the volume imaginary po-

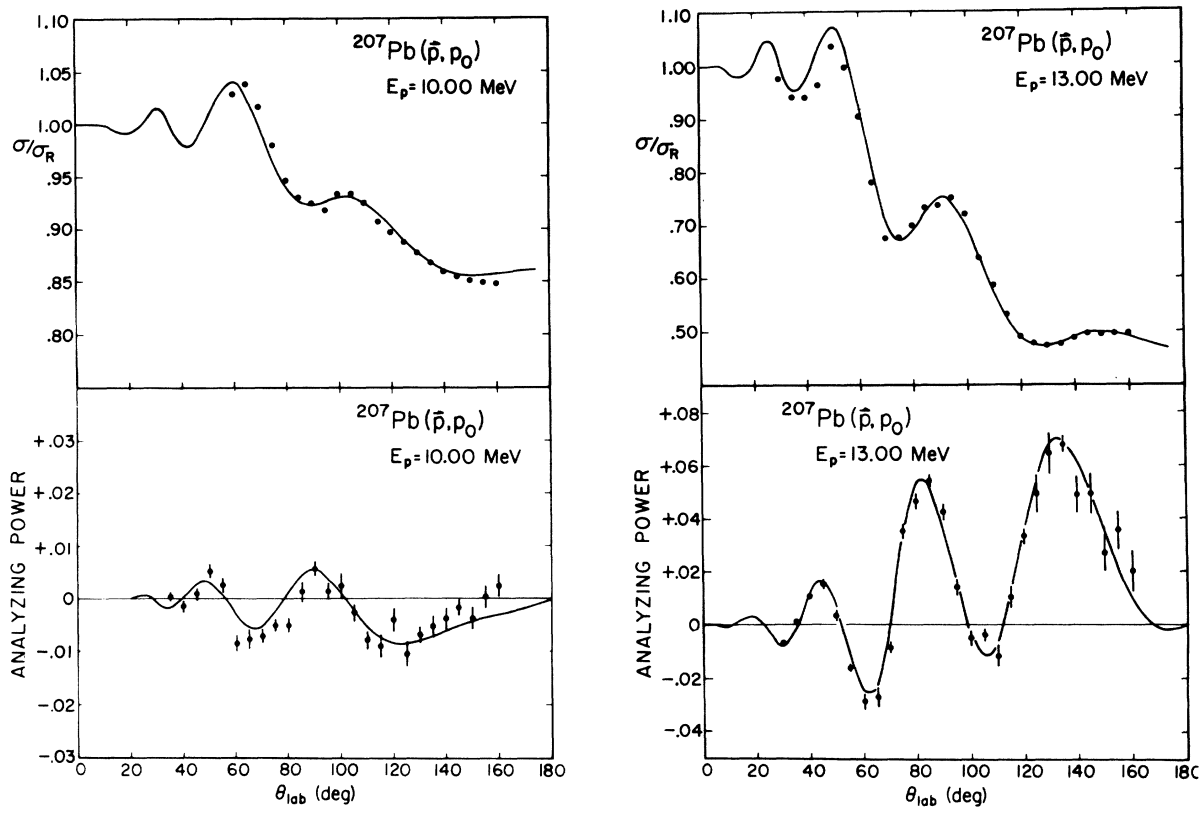

FIG. 5. Differential cross-section and analyzing-power angular distributions for $^{207}Pb(\vec{p},p_0)$ at two off-resonance energies, E_p=10.00 and 13.00 MeV. The curves are generated with the optical-model parameters in Table I.

tential W_v. The data used for the fitting included both differential cross sections and analyzing powers at both energies and at all angles (all angles $\geq 60°$ for ^{207}Pb). However, considerably more weight was given to the analyzing-power data. The program then minimized the total χ^2. The final results are shown in Table I and by the curves in Figs. 3 and 5. For both ^{206}Pb and ^{207}Pb, the nuclear phase shift $\lambda(p_{1/2})$ was found by interpolation to be about 4° in the vicinity of the resonance.

The excitation functions were analyzed using the program RESFIT, which minimizes χ^2 by varying only the resonance parameters. The optical model background and the higher-lying resonances remained fixed. Also, the total width of the IAR was fixed at a value determined from analysis of in-

TABLE I. Optical model parameters for $^{206}Pb(\vec{p},p_0)$ and $^{207}Pb(\vec{p},p_0)$.

	^{206}Pb	^{207}Pb
U (MeV)	$65.20-0.70*E_p$	$65.54-0.59*E_p$
r_R (fm)	1.26	1.26
a_R (fm)	0.69	0.67
W_{vol} (MeV)	0.	0.
W_{surf} (MeV)	$30.41-0.61*E_p$	$-7.00+1.80*E_p$
r_I (fm)	1.31	1.29
a_I (fm)	0.25	0.34
U_{so} (MeV)	4.47	5.81
r_{so} (fm)	1.15	1.13
a_{so} (fm)	0.63	0.65
r_c (fm)	1.19	1.19

TABLE II. Resonance parameters for the $3p_{1/2}$ isobaric analog resonances in ^{207}Bi* and ^{208}Bi*.

	^{207}Bi*	^{208}Bi*
I^π	$\frac{1}{2}^-$	0^+
ϵ_0 (MeV) (c.m.)	12.146 ± 0.007	11.458 ± 0.006
Γ_0 (keV)	170 ± 17	231 ± 6
Γ_{0p} (keV)	20 ± 2	51.6 ± 1.7
ϕ_p (deg.)	3 ± 2	−5 ± 2
Γ_{0p1} (keV)	7.5 (2^+, 0.803)	29.5 ± 4.0($\frac{5}{2}^-$, 0.57)
Γ_{0p2} (keV)	5.6 (0^+, 1.17)	66.8 ± 4.6($\frac{3}{2}^-$, 0.894)
Γ_{0p3} (keV)	9.4 (3^+, 1.34)	
Γ_{0p4} (keV)	21.1 (2^+, 1.47)	
Γ_{0p5} (keV)	15.4 (1^+, 1.71)	

elastic scattering data.[1,3] Thus the only parameters that were varied were the resonance energy ϵ_0, the elastic partial width Γ_{0p}, and the elastic mixing phase ϕ_p. (In what follows, we use the notation $\Gamma_{0c}=\Gamma_{0p}$, Γ_{0p1}, $\Gamma_{0p2},\ldots$, $\phi_c=\phi_p$, ϕ_{p1}, ϕ_{p2}, ..., to denote the widths and phases for decay to the ground state, first excited state, etc.) The data used in the search included essentially all the analyzing-power measurements, at all three angles, between $\epsilon_0-\Gamma_0$ and $\epsilon_0+\Gamma_0$. No cross section measurements were used. As mentioned above, the searches were done with several different sets of optical-model parameters, until a reasonable fit to all the data was obtained. The best fits were obtained with the parameters shown in Table II. The excitation functions generated with these parameters (and those in Table I) are shown in Figs. 2 and 4. The reduced χ^2's are 1.368 for ^{206}Pb and 1.034 for ^{207}Pb.

Also shown in Table II are the inelastic partial widths. These widths are adjustments to previously reported values.[1,3] The adjustments are necessary because the Γ_{0pi} are not measured directly in inelastic scattering experiments, but rather are inferred from the measured quantity $(\Gamma_{0pi}\Gamma_{0p}/\Gamma_0^2)$ and the values of Γ_{0p} and Γ_0. Since the values of Γ_{0p} determined in this work differ considerably from those reported previously, the values of Γ_{0pi} must be changed accordingly.

IV. DISCUSSION OF ERRORS

Potential sources of error include (a) systematic errors in the data, (b) statistical errors in the data, (c) uncertainty in the background parameters, and (d) other known errors (see below). (a) In the case of ^{207}Pb, there are several overlap points, including some for which the second measurement was made a month after the first one. An analysis of these points indicates that the scatter in the analyzing power is purely statistical. The low value of χ^2 tends to confirm this; the probability P_χ of exceeding a χ^2 of 1.034 due to statistical fluctuations is 39%. Therefore, for the ^{207}Pb data, systematic errors were not considered. For the ^{206}Pb data, it appears that they cannot be ignored. For one thing, P_χ is only 8%, so it seems likely that some nonstatistical factors were causing part of the scatter in the data. Also, there is very poor agreement between the measurements taken at 11.5 MeV for the angular distribution and those taken at the same energy for the excitation function. Nevertheless, the errors given in Table II do not include any contribution from systematic effects, and hence are probably too small in the case of ^{206}Pb. (b) The statistical error in the resonance parameters depends on the statistical error in the data points, the number of data points used, and the curvature of the χ^2 hypersurface near the minimum. The procedure used to determine the errors is given by Bevington[13]; the approximate effect of changing each parameter by its statistical error is an increase in the total χ^2 of 1. As a check on this error estimate, the following test was made. As mentioned above, the ^{207}Pb excitation functions are actually composites of two sets of data taken a month apart. A search was made on each data set separately, and the resulting parameter sets agreed with each other and with the "over-all" set to within the statistical error. (c) The errors due to the nonresonant background are difficult to determine quantitatively. To provide a basis for an error estimate, we generated different optical model sets, which gave small but noticeable degradations in the fit to the angular distributions, and found the optimum resonance parameters with respect to these sets. Typically, the resulting shifts in Γ_{0p} were negligible, but the shifts in ϵ_0 and ϕ_p were comparable to the statistical errors. (d) The error in ϵ_0 due to uncertainty in beam energy is estimated to be about 1 keV, and so can be ignored. Finally, we observe that the largest source of error in Γ_{0p} comes from the uncertainty in Γ_0, since the strength of the resonance is determined not by Γ_{0p} but by the ratio Γ_{0p}/Γ_0. The errors given in Table II include contributions from all the sources mentioned in (b), (c), and (d) above.

V. COMPARISON WITH *S*-MATRIX THEORY

In a recent paper,[14] Brentano discussed intermediate structure phenomena from an *S*-matrix viewpoint. His purpose was to describe intermediate structure resonances (such as IAR) as poles in the continued energy-averaged *S* matrix. Using very general assumptions, he found that in the vicinity of an isolated resonance the energy-averaged *S* matrix was given by

$$S_1(z)=S_{10}^{1/2}\left(1-i\frac{\gamma\times\gamma}{z-\epsilon_1}\right)S_{10}^{1/2}. \tag{10}$$

In this expression, $S_1(z)=S_1(E+iI)=\langle S(E)\rangle_I$ is the average *S* matrix at E with averaging interval I. The other matrices appearing in Eq. (10) are the background S_{10}, the unit matrix 1, and the residue $\gamma\times\gamma$ (whose elements are $\gamma_c\gamma_{c'}$). The quantities $\epsilon_1=E_1-\frac{1}{2}i\Gamma_1$ and $\gamma_c=\Gamma_c^{1/2}e^{i\phi_c}$ are complex. Brentano found that, as expected, the total width Γ_1 could be decomposed into an escape width and a spreading width: $\Gamma_1=\Gamma^\uparrow+\Gamma^\downarrow=\sum\Gamma_c\cos(2\phi_c)$. However, he also found that $\Gamma^\downarrow>\Gamma^\uparrow$, a restriction which does not appear in most theoretical approaches, and which implies that $\Gamma_1>2\sum\Gamma_c\cos(2\phi_c)$.

In the case where the background is diagonal, the elastic scattering matrix element reduces to

$$[S_1(z)]_{cc} = e^{2i(\delta_c + i\eta_c)}\left[1 - i\frac{\Gamma_c e^{2i\phi_c}}{z-\epsilon_1}\right]. \quad (11)$$

Comparing this to the expressions used in Sec. III, we see that $E_1 = \epsilon_0$, $\Gamma_1 = \Gamma_0$, and $\Gamma_c = e^{2\eta_c}\Gamma_{0c}$, so the inequality which needs to be verified is

$$\Gamma_0 > 2\sum_c \Gamma_{0c} e^{2\eta_c}\cos(2\phi_c) > 2\sum_c \Gamma_{0c}\cos(2\phi_c)\,, \quad (12)$$

since η_c is always positive.

Referring to Table II, and assuming that ϕ_c is approximately the same for all channels, we see that this inequality is satisfied for the $\frac{1}{2}^-$ IAR in ^{207}Bi, but not for the 0^+ IAR in ^{208}Bi. In fact, in the latter case, the value of $|\phi_c|$ that would be needed to make $\Gamma_0 = 2\sum_c \Gamma_{0c}\cos(2\phi_c)$ is $19^\circ \pm 2^\circ$, a value that is clearly inconsistent not only with what we report here but also with values of ϕ_p from similar experiments on medium-weight nuclei.[15]

Brentano gives a possible explanation for this discrepancy. In order to define the average S matrix in a reasonable way, he requires that the minimum averaging interval I_0 be large compared to both (a) the average distance between fine-structure resonances and (b) the width (Γ_j) of each of them. It must also be small compared to the widths and spacing of the intermediate-structure resonances. Under these assumptions, the average S matrix $S_1(z)$ will exhibit a smooth behavior in the lower half of the z plane ($I < -I_0$), with the only poles coming from the intermediate structure. Now the assumption that $I_0 \gg \Gamma_j$ is one that is usually not made in theoretical treatments of intermediate structure. For example, in the shell model approach,[6] it is possible to consider the limiting case in which the residual interaction does not mix the doorway state Φ_0 with the complicated states ϕ_j at all. In that case, there is only one "fine-structure" resonance, with a width equal to $\Gamma^\dagger$. As the strength of the coupling between Φ_0 and the ϕ_j increases, one approaches the other limiting case in which all the Γ_j's are of the same order of magnitude and $\sum_j \Gamma_j = \Gamma^\dagger$. Clearly, Brentano's treatment is well suited to the latter case but not to the former.

For the IAR, because of isospin selection rules, the mixing between the $T_>$ doorway state and the $T_<$ compound nuclear states is due primarily to the Coulomb interaction, and so is relatively small. It is therefore plausible that, even after mixing, there is one state which has a large $T_>$ component and therefore a large width. If this is so, then the requirement that $I_0 \gg \Gamma_j$ for all j cannot be satisfied.

Note also that in the shell-model approach $\Gamma^\dagger \approx v^2/d$, where v is the average matrix element connecting Φ_0 and ϕ_j, and d is the average level spacing. At high excitation energies in heavy nuclei, $1/d$ is very large. But if v^2 is sufficiently small, as in the IAR, it is nevertheless possible to have $\Gamma^\downarrow$ comparable to $\Gamma^\dagger$. In fact, we observe that $\Gamma^\downarrow \approx \Gamma^\dagger$ in ^{207}Bi, while in ^{208}Bi we have $\Gamma^\downarrow < \Gamma^\dagger$.

VI. CONCLUSION

This study of the elastic-scattering analyzing power in two Pb nuclei near the lowest-lying IAR's shows the value of such measurements for determining the resonance parameters. Even though the resonance effect is small, it is still possible to observe and parametrize it because of the even smaller background. For the differential cross section, on the other hand, the resonance appears as a small bump on a very large Rutherford-scattering background. Therefore, a more accurate determination of Γ_{0p} can be made using analyzing-power data. It turns out that the values of Γ_{0p} determined in these experiments are not very sensitive to the choice of background parameters; they are also considerably different from the values determined from cross-section data. Hence this technique is capable of producing more spectroscopic information on the parent states. Another advantage of this method is that it gives a more accurate value for the mixing phase ϕ_p (Ref. 16); however, this value is more sensitive than Γ_{0p} to the parametrization of the background.

It appears, at least in the case of the 0^+ IAR in ^{208}Bi, that Brentano's description of the IAR as a pole in the continued energy-averaged S matrix is not a very useful one. This approach requires a degree of mixing between the doorway state and the complicated states which is not always present in the IAR, where the mixing is inhibited by isospin selection rules. While the theory gives the correct form for the average S matrix, it also makes a prediction about the resonance parameters which is not verified in this case.

ACKNOWLEDGMENTS

This research was supported by the Energy Research and Development Administration. We wish to thank Professor J. S. Blair and Professor W. G. Weitkamp for their assistance during the early stages of this research.

*Present address: Los Alamos Scientific Laboratory, University of California, Los Alamos, New Mexico.

[1]C. D. Kavaloski, J. S. Lilley, P. Richard and N. Stein, Nuclear Physics Laboratory Annual Reports, University of Washington, 1965 (unpublished), p. 1; 1967 (unpublished), p. 18.

[2]G. H. Lenz and G. M. Temmer, Nucl. Phys. A112, 625 (1968).

[3]E. C. Booth and B. S. Madsen, Nucl. Phys. A206, 293 (1973).

[4]G. Graw, in *Polarization Phenomena in Nuclear Reactions*, edited by H. H. Barschall and W. Haeberli (University of Wisconsin Press, Madison, Wisconsin, 1971), p. 179.

[5]See AIP document No. PAPS PRVCA-17-2053-11 for 11 pages of tabulated data on analyzing power excitation functions and angular distributions. Order by PAPS number and journal reference from American Institute of Physics, Physics Auxiliary Publications Service, 335 East 45th Street, New York, New York 10017. The price is $1.50 for microfiche or $5 for photocopies. Airmail additional. Make checks payable to the American Institute of Physics. This material also appears in *Current Physics Microfilm*, the monthly microfilm edition of the complete set of journals published by AIP, on frames immediately following this journal article.

[6]C. Mahaux and H. A. Weidenmüller, *Shell-model Approach to Nuclear Reactions* (North-Holland, Amsterdam, 1969).

[7]The phase of P_l^m is that given in E. U. Condon and G. H. Shortley, *Theory of Atomic Spectra* (Cambridge U. P., Cambridge, 1953). Many authors define P_l^1 with the opposite sign.

[8]F. D. Becchetti and G. W. Greenlees, Phys. Rev. 182, 1190 (1969).

[9]R. D. Rathmell and W. Haeberli, Nucl. Phys. A178, 458 (1972).

[10]F. G. Perey, Oak Ridge National Laboratory (unpublished).

[11]M. P. Baker, J. S. Blair, J. G. Cramer, E. Preikschat, and W. Weitkamp, in *Proceedings of the Fourth International Symposium on Polarization Phenomena in Nuclear Reactions*, edited by W. Grüebler and V. König (Birkhäuser, Basel, 1976), p. 781.

[12]K. Ramavataram, S. Ramavataram, W. G. Davies, A. J. Ferguson, and J. S. Fraser, Phys. Rev. C 10, 632 (1974).

[13]P. R. Bevington, *Data Reduction and Error Analysis for the Physical Sciences* (McGraw-Hill, New York, 1969).

[14]P. von Brentano, in *Proceedings of the Europhysics Study Conference on Intermediate Processes in Nuclear Reactions*, edited by N. Cindro (Springer, New York, 1973), p. 267.

[15]The values of ϕ_p reported here are also inconsistent with those calculated using a modified R-matrix theory; cf. W. J. Thompson, Nucl. Data A6, 129 (1969).

[16]The accurate determination of ϕ_p is helped by the choice of a scattering angle (120° in this case) where the analyzing-power resonance dispersion shape is approximately antisymmetric about ϵ_0. In that case, it can be shown that $A(E,\theta)$ is linear in ϕ_p for small ϕ_p, with the maximum variation at $E=\epsilon_0$. If the shape were symmetric about ϵ_0, $A(E,\theta)$ would also be linear in ϕ_p, but the maximum variation would occur at $E=\epsilon_0 \pm \frac{1}{2}\Gamma_0$ and would be only half as large.